LBNL-47900
Preprint

ERNEST ORLANDO LAWRENCE
BERKELEY NATIONAL LABORATORY

van der Waals Theory for Fluid-Solid Equilibria of Chain-Like Molecules

Nicola Elvassore and John M. Prausnitz

Chemical Sciences Division

May 2001

Submitted to
Fluid Phase Equilibria

REFERENCE COPY
Does Not
Circulate

LBNL-47900
Copy 1

Library Annex Reference
Lawrence Berkeley National Laboratory

DISCLAIMER

This document was prepared as an account of work sponsored by the United States Government. While this document is believed to contain correct information, neither the United States Government nor any agency thereof, nor the Regents of the University of California, nor any of their employees, makes any warranty, express or implied, or assumes any legal responsibility for the accuracy, completeness, or usefulness of any information, apparatus, product, or process disclosed, or represents that its use would not infringe privately owned rights. Reference herein to any specific commercial product, process, or service by its trade name, trademark, manufacturer, or otherwise, does not necessarily constitute or imply its endorsement, recommendation, or favoring by the United States Government or any agency thereof, or the Regents of the University of California. The views and opinions of authors expressed herein do not necessarily state or reflect those of the United States Government or any agency thereof or the Regents of the University of California.

LBNL-47900

van der Waals Theory for Fluid-Solid Equilibria of Chain-Like Molecules

Nicola Elvassore[1] and John M. Prausnitz[2]

[1]Dipartimento di Principi e Impianti di Ingegneria Chemica
DIPIC
Università di Padova
Via Marzolo, 9 I-35100 Padova, Italy

[2]Department of Chemical Engineering
University of California, Berkeley
and
Chemical Sciences Division
Ernest Orlando Lawrence Berkeley National Laboratory
University of California
Berkeley, California 94720

May 2001

This work was supported by the Director, Office of Science, Office of Basic Energy Sciences, Chemical Sciences Division, of the U.S. Department of Energy under Contract No. DE-AC03-76SF00098.

van der Waals Theory for Fluid-Solid Equilibria of Chain-Like Molecules

Nicola Elvassore[1+] and John M. Prausnitz[2*]

[1] Dipartimento di Principi e Impianti di Ingegneria Chimica, DIPIC, Università di Padova,
Via Marzolo, 9 I-35100 Padova, Italy
E-mail nicola.elvassore@unipd.it
phone: +39-049-827-5469 fax: +39-049-827-5461

[2] Department of Chemical Engineering, University of California,
and Chemical Sciences Division, Lawrence Berkeley National Laboratory,
Berkeley, CA 94720 USA
E-mail prausnit@cchem.berkeley.edu
phone: +1-510-642-3592 fax: +1-510-642-4778

Original Manuscript

Submitted for publication in *Fluid Phase Equilibria*

* Author to whom correspondence should be addressed; + Presenting author

Abstract

Van der Waals perturbation theory is used to calculate fluid-solid phase diagrams for a system of perturbed-hard-sphere chains. In both fluid and solid phases, the free energy is the sum of a hard-sphere-chain term as the reference system, and a van der Waals term as the perturbation. The reference system for both phases follows from the Percus-Yevick integral theory coupled with Chiew's results for hard chains. An analytic model for the solid-phase reference term of a hard-chain system agrees well with computer-simulation data for the solid hard-chain compressibility. Simulation data for fluid-solid coexistence curves for hard spheres, and for 4-mer hard chains, are used to fit the reference Helmholtz free energy of the solid phase. The pressure and solid- and fluid densities at the hard-chain melting point, predicted by our model, fairly reproduce the available simulation data at different chain lengths.

The attractive perturbation term follows from an inverse-power potential with variable exponent n for both fluid and solid phases. The theory here presented reproduces the simulated phase diagrams of chain-like molecules and gives the correct trend for experimental melting points of normal alkanes.

(Keywords: van der Waals theory; solid-fluid equilibria; phase diagram; chain-like molecules)

Introduction

In recent years, there has been much interest in understanding the effects of molecular size and shape on solid-fluid equilibria. Solid-liquid equilibria for asymmetric and chain-like molecules are of interest for industrial applications such as wax precipitation in petroleum systems [1] or polymer precipitation by liquid or compressed-gas antisolvents [2].

Several models have been proposed previously. Some of these use modifications of regular-solution theory of mixtures as well as an equation of state [3,4,1]. However, application of these models requires the fugacity of the solid, as obtained from the following pure-component properties: the triple (or melting) temperature, heat capacity and molar volume of both fluid and solid phases, and the enthalpy of fusion at the triple point.

On the other hand, the solid-phase equation of state can be derived from a van der Waals perturbation theory. Although this theory is based on simple ideas, it can be used not only for fluid-fluid phase calculations, as intended originally, but also for fluid-solid phase equilibria. Unfortunately, the only reported analytical equations of state for a solid are for hard spheres [5-7].

To understand the solid-fluid phase behavior of a hard-sphere-chain system, molecular simulations of these systems were recently presented [8-11]. The simulation data are only applicable to the simulated chain length.

In this work, we develop an analytic theory for describing the solid phase of perturbed-hard-sphere-chain systems. The model here proposed is of general applicability; both fluid and solid equations of state are functions of the number of chain segments. Although the model gives only a crude description of the solid perturbed-hard-sphere-chain system, it provides a phenomenological description of chain-length effects on the thermodynamic properties of both the fluid and the solid phase.

Theoretical framework

Both fluid and solid reference systems are modeled by a chain of r-freely-jointed tangent spheres. Attractive interactions are given by a perturbation mean-field potential. The pressure follows from three contributions: a nonbonding contribution (i.e. hard spheres before bonding to form the chain), a bonding contribution due to chain formation (hard chain) and a perturbation contribution to account for attraction (dispersion forces). Contrary to the perturbation contributions; the reference terms in both fluid and solid phases do not take chain connectivity into account.

Dimensionless equations are used for convenience. The dimensionless variables are:

$$\tilde{p} = \frac{p}{\rho_0 \varepsilon} \qquad \tilde{T} = \frac{k_B T}{\varepsilon} \qquad \eta = \frac{\pi r \rho \sigma^3}{6} \tag{1.}$$

where ρ is the molecular density, r is the number of segments, σ is the hard-sphere diameter, ε is the potential energy parameter, ρ_0 is the one-particle density (reciprocal volume of one particle), k_B is Boltzmann's constant and $\tilde{p}$, $\tilde{T}$ and, η are respectively, the reduced pressure, the reduced temperature and the segment packing fraction.

To derive the reference hard-sphere-chain equation of state for both fluid and solid phases, we use results from Chiew [12] and from Song et al. [13] where the Percus-Yevick integral equation of state is coupled with chain connectivity. A generalized Chiew's equation of state is represented by the radial distribution function of hard spheres at contact. The reference compressibility factor of the hard-sphere chain can be rearranged in a general form [13]:

$$z_{ref} = \left(\frac{p}{\rho k T}\right)_{ref} = 1 + 4r\eta g(d^+) - (r-1)\left[g(d^+) - 1\right] \tag{2.}$$

where $g(d^+)$ is the radial distribution function of hard spheres at contact, prior to bonding to form the chains. Here, d is the effective hard-sphere diameter.

The reference Helmholtz free energy A, obtained by integrating [14] the compressibility factor z_{ref} of Eq. (2), can be written in the general form for a one-component system:

$$\left(\frac{A}{Nk_BT}\right)_{ref} = \frac{A^0}{Nk_BT} + 4r\eta W + (r-1)Q + \ln\eta \tag{3.}$$

where A^0 is the reference Helmholtz energy, while W and Q are defined by:

$$W = \frac{1}{\rho}\int_0^{\rho} g(d^+)d\rho \tag{4.}$$

$$Q = \int_0^{\rho}\left(g(d^+)-1\right)\frac{d\rho}{\rho} \tag{5.}$$

These expressions hold for both liquid and solid phases. However, each phase requires an explicit expression for the radial distribution function $g(d^+)$. Details are reported in the following section.

The perturbation term for both equations of state is derived from a simple potential. We assume that spheres interact through an attractive inverse-power potential (generalized Sutherland Potential):

$$u(\tilde{R}) = \begin{cases} \infty & \tilde{R} < 1 \\ -\varepsilon/\tilde{R}^n & 1 \le \tilde{R} \end{cases} \tag{6.}$$

where $\tilde{R} = R/\sigma$ is the reduced center-to-center distance between spheres, R is center to center distance of spheres and n is a positive constant. Upon varying n, it is possible to change the interaction range; increasing n reduces the range of attractive interaction.

Expressions for the equation of state and Helmholtz free energy are obtained by combining the reference and the perturbation terms of each equation as derived from the van der Waals perturbation theory in the following sections. The fluid-fluid and fluid-solid coexistence curves for a pure fluid are calculated by equating the reduced pressure and the chemical potential of the coexisting phases at the same temperature.

Equations of state and thermodynamic functions

Fluid phase

For the fluid phase, the radial distribution function was derived from the Carnahan-Starling [15] equation. The reference equation of state (Eq. 2) and the integration of W and Q for the Helmholtz free energy reference term (Eq. 3) are reported elsewhere [13] for the fluid phase.

The Helmholtz free energy perturbation term of the fluid phase is proportional to the product of the number density and the average pair potential evaluated over the center-to-center intermolecular distance. The van der Waals perturbation term for the Helmholtz free energy, derived using the inverse power potential [5], gives two identical expressions:

$$\left(\frac{p}{\rho k_B T}\right)_{pert} = -r\frac{\eta}{\tilde{T}}\frac{12}{n-3} \qquad (7.)$$

$$\left(\frac{A}{N k_B T}\right)_{pert} = -r\frac{\eta}{\tilde{T}}\frac{12}{n-3} \qquad (8.)$$

Solid Phase

The results from Chiew [12] and from Song et al. [13] were rearranged using a model for the radial distribution function appropriate for hard spheres in a solid.

We use a simple expression for the radial distribution function of hard spheres, based on the model proposed by Daanoun et al. [5]:

$$g(d^+) = \frac{1}{(1-\delta)\delta^2}\frac{1}{4\eta_{cp}} \qquad (9.)$$

where δ is the inverse of the reduced distance between two solid-phase particles given by:

$$\delta = \left(\frac{\eta_s}{\eta_{cp}}\right)^{1/3} \qquad (10.)$$

Here η_{cp} is the maximum value of the density at close pacing (cp) of the given lattice structure. This value depends on the crystal structure. We use a face-centered cubic (fcc) structure with

η_{cp}=0.74048 and a coordination number, z_{latt} of the corresponding lattice equal to12. Substitution of Eqs. (9) and (10) in Eq. (2) gives the compressibility factor for hard-sphere chains in the solid phase.

The fluid-solid phase equilibrium calculations require an expression for the Helmholtz free energy of the solid phase. Integration of W and Q from zero density is not obvious. It is of fundamental importance that both the fluid and the solid Helmholtz energy have the same reference state. To obtain an expression for W, it may be possible to integrate Eq. (4) from zero density to solid density by adding the contribution of the communal entropy [16]. However, Eq (9) is accurate only at high density and the free energy derived from the ideal-gas integral gives an erroneous hard-sphere melting point. According to Monte Carlo simulation data for solid-fluid equilibrium, a constant c_{01} has been adjusted to reproduce the simulated melting pressure. The fluid and solid densities at melting conditions were predicted by:

$$W = -\frac{3}{4\eta_{CP}}\frac{\ln(1-\delta)}{\delta^3} + c_{01} \qquad (11.)$$

with $c_{01} = -0.4784$. For r>1, a second constant was added to Q for the reference Helmholtz energy to reproduce the simulated 4-mer hard-sphere-chain melting pressure [8] Eq (5) becomes:

$$Q = -3\ln(\delta) + \frac{3}{4\eta_{cp}}\left[\ln\frac{\delta}{1-\delta} - \frac{1}{\delta} - \frac{1}{2\delta}\right] + c_{02} \qquad (12.)$$

with $c_{02} = 1.1575$.

For the solid-phase perturbation term we follow the model based on the lattice structure that represents a solid phase as a perfect crystal. In this case the perturbation term for the Helmholtz free energy is proportional to the product of lattice coordination number z_{latt} and the pair potential evaluated at the system's intermolecular separation distance.

For the solid-phase perturbation term we use the cell theory combined with the inverse-power potential [5]. The Helmholtz perturbation energy can be expressed by the sum over spherical shells of sites centered around the site at the origin. Applying the pair potential to the first lattice shell

containing z_{latt} sites for each segment of the chain, the perturbation Helmholtz energy and compressibility factor are given by:

$$\left(\frac{A}{Nk_BT}\right)_{pert} = -r\frac{z_{latt}}{2}\frac{\varepsilon}{k_BT}\frac{1}{\widetilde{R}^{n_{IP}}} \tag{13.}$$

$$\left(\frac{p}{\rho k_BT}\right)_{pert} = -r\frac{z_{latt}n_{IP}}{6}\frac{\varepsilon}{k_BT}\frac{1}{\widetilde{R}^{n}} \tag{14.}$$

where $\widetilde{R}$ is the average reduced distance between closest neighbors in the lattice.

Results and discussion

This section discusses the features of the model for the solid hard-sphere chain and for solid-fluid equilibrium. For all systems studied, calculated results are compared with those from Monte Carlo simulations.

Figure (1) shows the calculated compressibility factor and the simulation data of Malanoski and Monson [8] for a system of hard-sphere chains. The model predicts the theoretical behavior of the chains as a function of number of segments. Unfortunately, because simulation data are available only for short chains (8 *mers*), it is not possible to test the model for longer chain molecules. Although Chiew's theory can be considered exact only at low density, agreement with simulation data can be considered satisfactory for developing a practical equation of state for a solid.

Figure (2) shows a comparison of calculated liquid and solid compressibility factors with simulation data [8]. The integration constants, c_{01} and c_{02}, fairly reproduce the melting pressure of the 4-mer chain. The model predicts the hard-chain reduced densities at equilibrium conditions for both fluid and solid phases. The fluid reduced density is stable up to the freezing value 0.54, whereas the corresponding reduced density value of the solid phase is 0.60 for the fcc lattice. These results are consistent with computer-simulation data [8] that give fluid and solid reduced densities stable at least up to 0.52 and 0.59, respectively.

Table 1 presents a summary of calculated and predicted hard-sphere-chains melting points for chains of 2, 4, 6 and 8 segments. The model predicts the solid-liquid equilibrium pressure up to an 8-mer hard-sphere chain (maximum chain length available in open literature) within 2% error, indicating that the integration constants c_{01} and c_{02} may be considered independent of chain length. The fluid and solid density predictions at the melting point are reproduced by the model for all considered chain lengths. A slight overestimation of both densities appears due to approximations in Chiew's theory.

It is well known that in any equilibrium calculation the important parameter is the one that specifies the range of attractive interaction. As shown by Hino and Prausnitz [7], where the solid van der Waals theory was applied to protein systems, varying the exponent n of the inverse-power potential gives different phase diagrams. Figure (3) shows a typical example for hard spheres corresponding to n=5 in Fig. (3a) and to n=6 in Fig. (3b), respectively. The position of the fluid-fluid critical point does not change. However, upon increasing the exponent of the inverse power potential, the triple point moves to lower density. The same behavior was observed for the phase diagram of hard-sphere chains.

To represent chain-like molecules we assume n=5. Figure (4) shows how the phase diagram changes upon increasing the number of segments in the chain. These results are qualitatively representative of the phase behavior of chain-like molecules. For all chain lengths considered, the ratio between the critical and triple temperature is around 0.4, similar to that for normal alkanes.

Figure (5) shows the p-T phase diagram for two different chains; results are consistent with simulation data reported by Polson and Frenkel [9]. A quantitative comparison of the two results is not possible because Polson and Frenkel use different interaction potentials.

Figure (6) shows the reduced melting-point temperature versus the number of segments at different pressures; these results fairly reproduce the trend of the experimental melting-point temperatures for n-alkanes.

The simple inverse-power potential used in this work does not allow us to represent the experimental normal melting point of alkanes with one value of the segment-segment interaction parameter, ε. Probably better results may be obtained using a more sophisticated soft-core potential. The average reduced distance for the solid phase hard-sphere chain at melting point is around 1.10 (the minimum of the Lennard-Jones potential is 1.12). In this region the segments are close together and their interactions are poorly described by our oversimplified potential.

Conclusions

An analytic theory was derived to describe the solid phase. Applicability of this model requires only properties of the molecules expressed by the potential of the chains. Results obtained here may be modified by using any suitable segment-segment potential.

The analytic equations shown here give a reasonable description of solid-phase properties; good agreement between the model and simulation data for hard-sphere chains was found. Solid and fluid densities at equilibrium for hard-sphere chains are predicted with satisfactory accuracy. The qualitative solid-fluid phase diagram reproduces the trend of the experimental melting-point temperatures for *n*-alkanes.

Phase-diagram predictions and the behavior of the melting point as a function of the number of segments, although qualitatively correct, are limited by the accuracy of the perturbation term based on the attractive mean-field approximation. Improvement may be obtained through a more accurate perturbation term or through a solid reference term that takes into account softness of the segment diameter.

Acknowledgment

This work was partially supported by the Italian Ministero dell'Università e della Ricerca Scientifica e Tecnologica (*ex-40%*) and by the Office of Basic Energy Sciences of the US Dept. of Energy.

List of Symbols

A	Helmholtz free energy
d	effective hard-sphere diameter
$g(d^+)$	radial distribution function
k_B	Boltzmann's constant
n	exponent of the inverse power potential
p	pressure
$\tilde{p}$	reduced pressure
r	number of segments
R	center to center distance
$\tilde{R}$	reduced center-to-center distance
T	absolute temperature
$\tilde{T}$	reduced temperature
z	compressibility factor
z_{latt}	lattice coordination number

Greek

δ	inverse of the reduced distance
ε	potential energy parameter
ρ	molecular density
ρ_0	one-particle density
η	segment packing fraction
η_{cp}	packing fraction at close pacing
σ	hard-sphere diameter

References and notes

[1] Lira-Galeana, C., A. Firoozabadi, J. M. Prausnitz, AIChE J., 42 (1996) 239-248.

[2] Jessop P. G., W. Leitner Eds, "Chemical Synthesis Using Supercritical Fluids", Wiley-VCH, Wenheim, Germany, 1999.

[3] Countinho, J. A. P., I. S. Andersen, E. H. Stenby, Fluid Phase Equilb., 103 (1995) 23-39.

[4] Harismiadis, V. I., D. P. Tassios, Ind. Chem. Eng. Res, 35 (1996) 4667-4681.

[5] Daanoun, A., C. F. Tejero, and M. Baus, Phys. rev. E, 50 (1994) 2913-2924.

[6] Young, D. A, J. Chem. Phys., 98 (1993) 9819-9829.

[7] Hino, T., J. M. Prausnitz, AIChE J., 45 (1999) 622-632.

[8] Malanoski, A. P., P. A. Monson, J. Chem. Phys., 107 (1997) 6899-6907.

[9] Polson, J. M., D. Frenkel, J. Chem. Phys., 109 (1998) 318-328.

[10] Malanoski, A. P., P. A. Monson, J. Chem. Phys., 110 (1999) 664-675.

[11] Malanoski, A. P., C. Vega, P. A. Monson, Molecular. Phys., 98 (2000) 363-370.

[12] Chiew, Y. C., Mol. Phys., 70 (1990) 129-143.

[13] Song, Y., S. M. Lambert, and J. M. Prausnitz, Ind. Chem. Eng. Res, 33 (1994) 1047-1057.

[14] J.M. Prausnitz, R.N. Lichtenthaler, E.G. de Azevedo, "Molecular Thermodynamics of Fluid-Phase Equilibria", 3rd Ed., Prentice Hall, NJ, 2000.

[15] Carnahan, N. F., K. E. Starling, J. Chem. Phys., 51 (1969) 635-636.

[16] Hoover, W. G., F. H. Ree, J. Chem. Phys., 49 (1968) 3609-3617.

[17] Dickman, R. and C. Hall, J. Chem. Phys., 89 (1988) 3168-3178.

Tables

Table 1.

Comparison between simulated and calculated hard-sphere-chain melting points. Simulation data for hard spheres from Hoover and Ree [16]; hard-sphere chains from Malanoski and Monson [8]; [p] data from our model; [c] data used to fit integration constants c_{01} and c_{02}.

	Simulated data			**Calculated data**		
r	η_F	η_S	$\frac{pr\sigma^3}{k_BT}$	η_F	η_S	$\frac{pr\sigma^3}{k_BT}$
1	0.494	0.545	11.7	0.493	0.556	11.7[c]
3	0.529	0.591	39.6	0.541	0.602	38.3[p]
4	0.529	0.591	52.1	0.549	0.608	52.1[c]
6	0.539	0.602	82.2	0.557	0.615	80.0[p]
8	0.539	0.602	107.5	0.561	0.618	108.1[p]

η_F and η_S are the segment packing fractions for the fluid and solid phase, respectively.

Figure captions

Figure 1. The hard-sphere-chain compressibility factor ($\beta p/\rho$) vs the segment packing fraction ($r\pi\rho\sigma^3/6$) curves for different chain lengths. The curves lie in sequence with n=1 having the lowest pressures. For the solid phase, the points are simulation result for chains of 1, 4 and 8 segments proposed by Malanoski and Monson [8]; the lines are predictions of the model proposed in this work. Here $\beta=(k_BT)^{-1}$.

Figure 2. Fluid and solid hard-sphere-chain compressibility factor ($\beta p/\rho$) vs segment packing fraction ($r\pi\rho\sigma^3/6$) for the 4-mers hard-sphere chain. The points are Monte Carlo simulation results. Full circles are data from Malanoski and Monson [8]; open circles are from Dickman and Hall [17]. The line connecting the two branches (F=fluid; S=solid) marks the equilibrium coexistence pressure of 4-mer hard-sphere chains. Here $\beta=(k_BT)^{-1}$.

Figure 3. Theoretical diagrams showing reduced temperature (k_BT/ε) vs segment packing fraction ($r\pi\rho\sigma^3/6$) for a perturbed-hard-sphere system with different power potential: (a) n=5 and (b) n=6. The model for the solid phase (S) is based on a fcc lattice and in part (b) the broken curve is the coexistence curve for fluid-fluid (F) equilibria.

Figure 4. Theoretical diagrams for reduced temperature (k_BT/ε) vs segment packing fraction ($r\pi\rho\sigma^3/6$) for perturbed-hard-sphere chains of different lengths with n=5 (F=fluid; S=solid). The model for the solid phase is based on an fcc lattice. Curves for different chain lengths lie in sequence with r=1 having the lowest pressure. This figure shows both fluid-fluid and solid-fluid equilibria for chains of 1, 2 and 4 segments.

Figure 5. Theoretical phase diagrams showing reduced pressure ($p\sigma^3/\varepsilon$) vs reduced temperature (k_BT/ε) for perturbed-hard spheres and for 4-mer perturbed-hard-sphere

chains with n=5 (F=fluid; S=solid): (a) solid-fluid coexistence curve and (b) solid-fluid-fluid coexistence curves for 1-mer and 4-mer hard-sphere chains.

Figure 6. Melting-point temperature of perturbed-hard-sphere chains vs number of segment of the chain, r, at two different reduced-pressures.

Figure 1

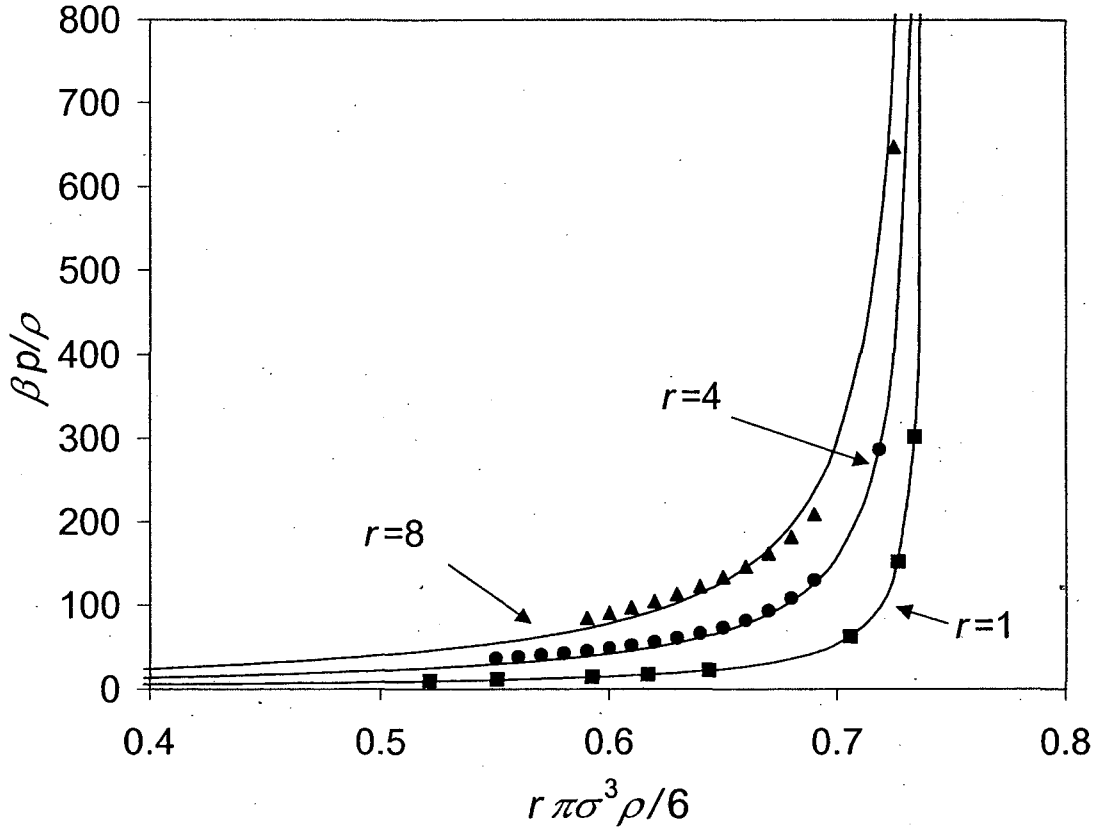
800
700
600
500
400
300
200
100
0
$\beta p/\rho$
0.4
0.5
0.6
0.7
0.8
$r\pi\sigma^3\rho/6$
r=4
r=8
r=1

Figure 2

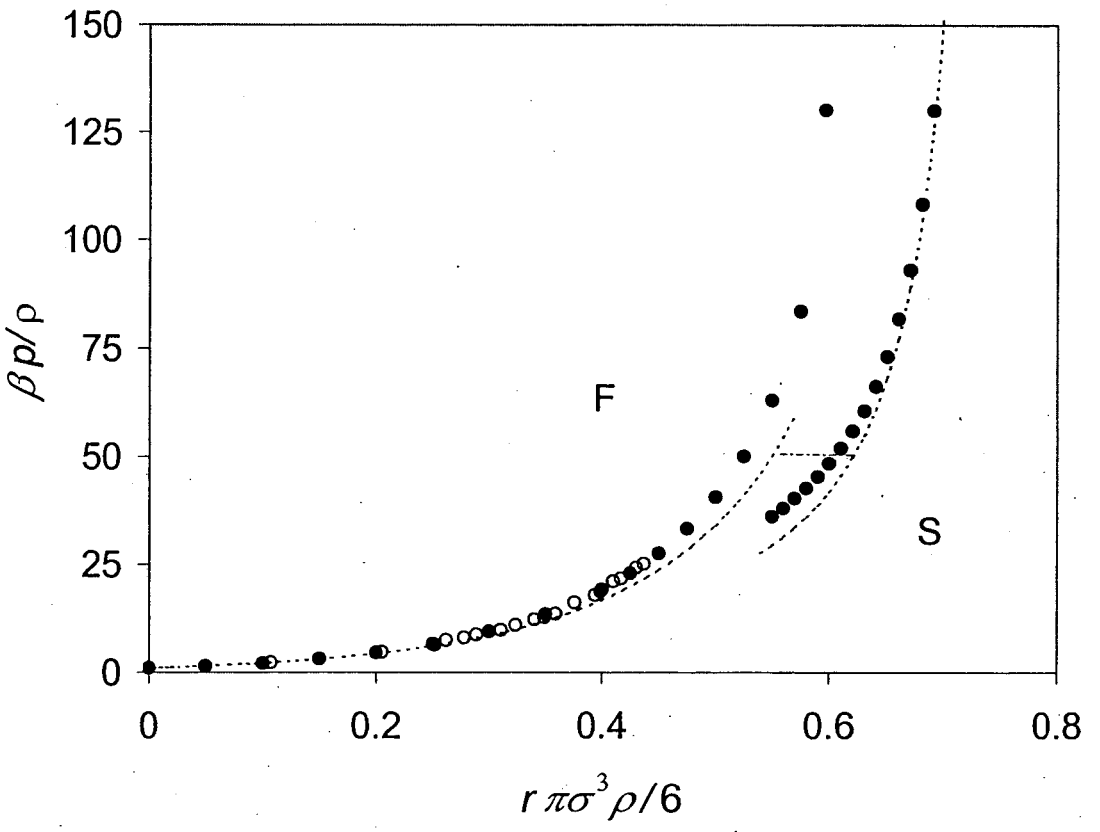

Figure 3

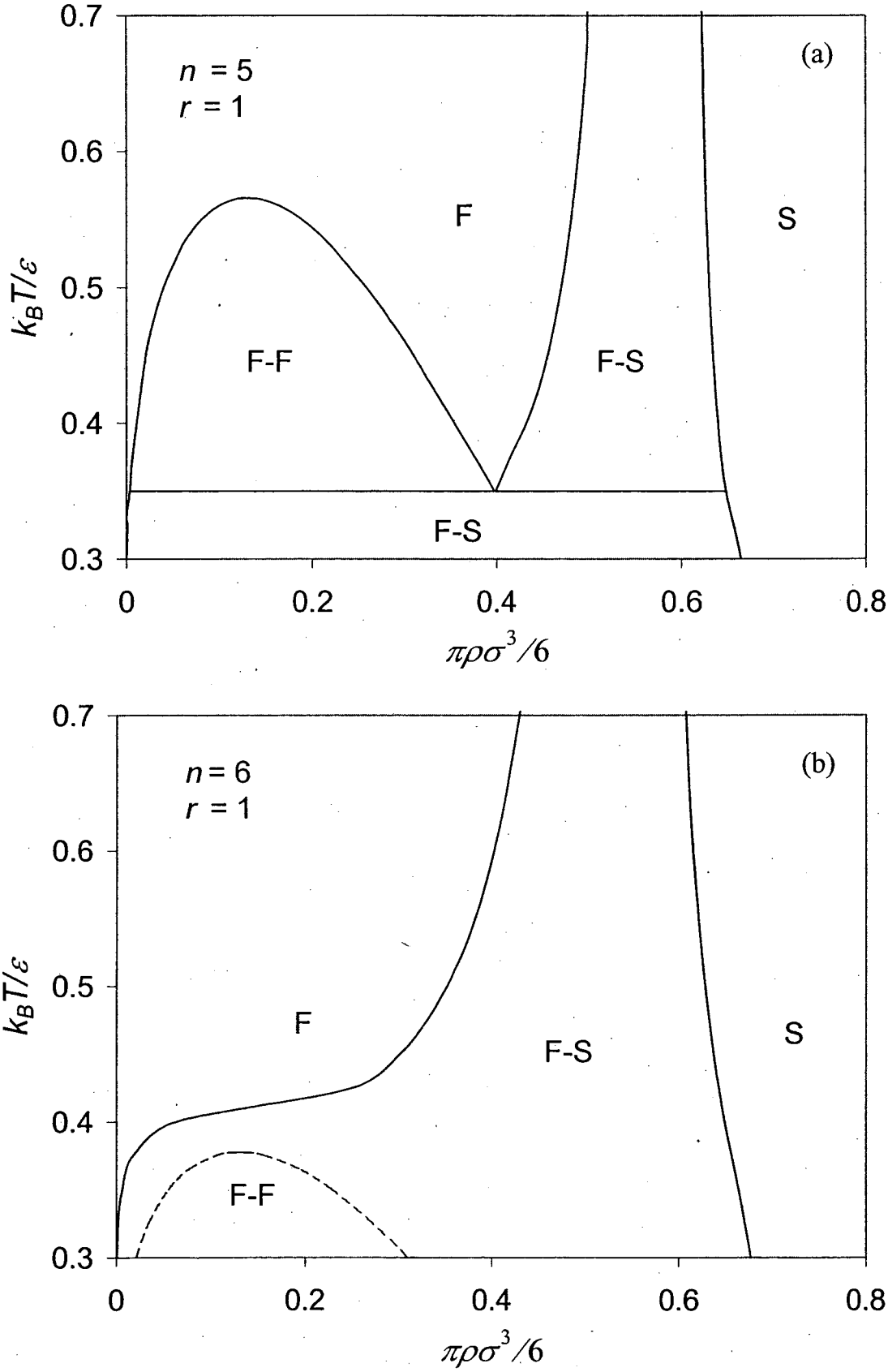
0.7
0.6
0.5
0.4
0.3
$k_B T/\varepsilon$
$n = 5$
$r = 1$
(a)
F
S
F-F
F-S
F-S
0
0.2
0.4
0.6
0.8
$\pi\rho\sigma^3/6$
0.7
0.6
0.5
0.4
0.3
$k_B T/\varepsilon$
$n = 6$
$r = 1$
(b)
F
F-S
S
F-F
0
0.2
0.4
0.6
0.8
$\pi\rho\sigma^3/6$

Figure 4

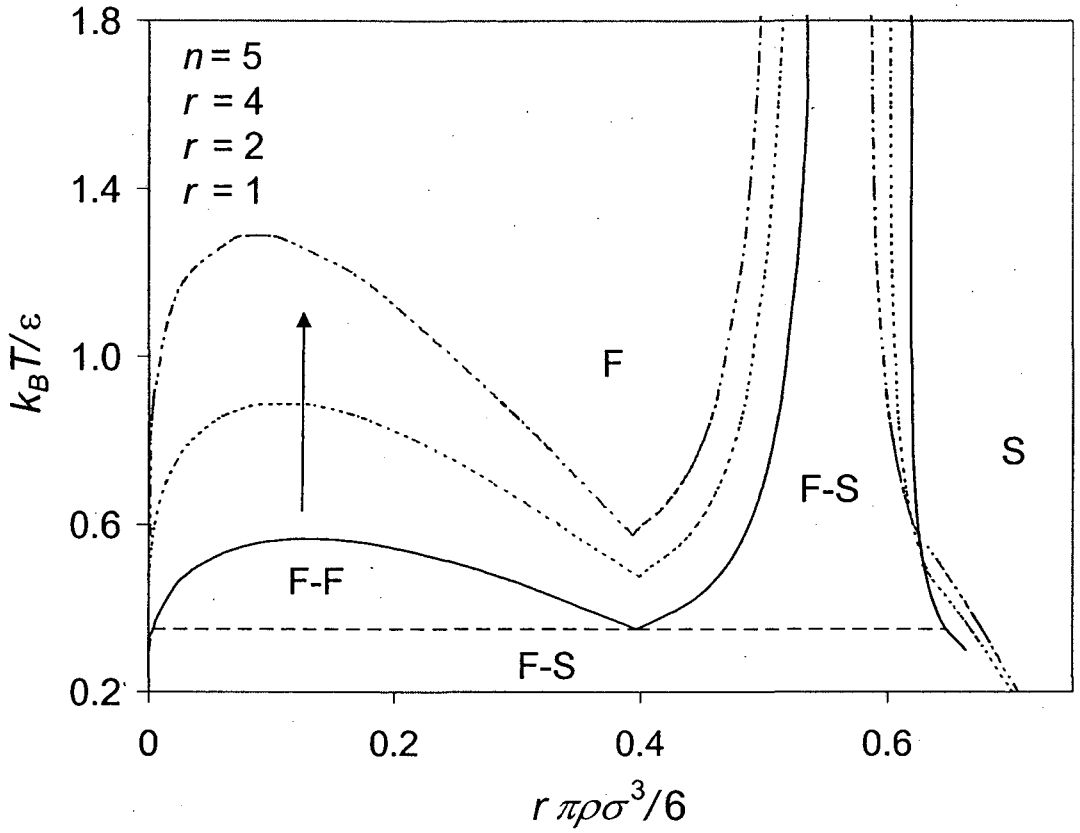
1.8
1.4
1.0
0.6
0.2
$k_B T/\varepsilon$
$n = 5$
$r = 4$
$r = 2$
$r = 1$
F
F-F
F-S
F-S
S
0
0.2
0.4
0.6
$r\,\pi\rho\sigma^3/6$

Figure 5

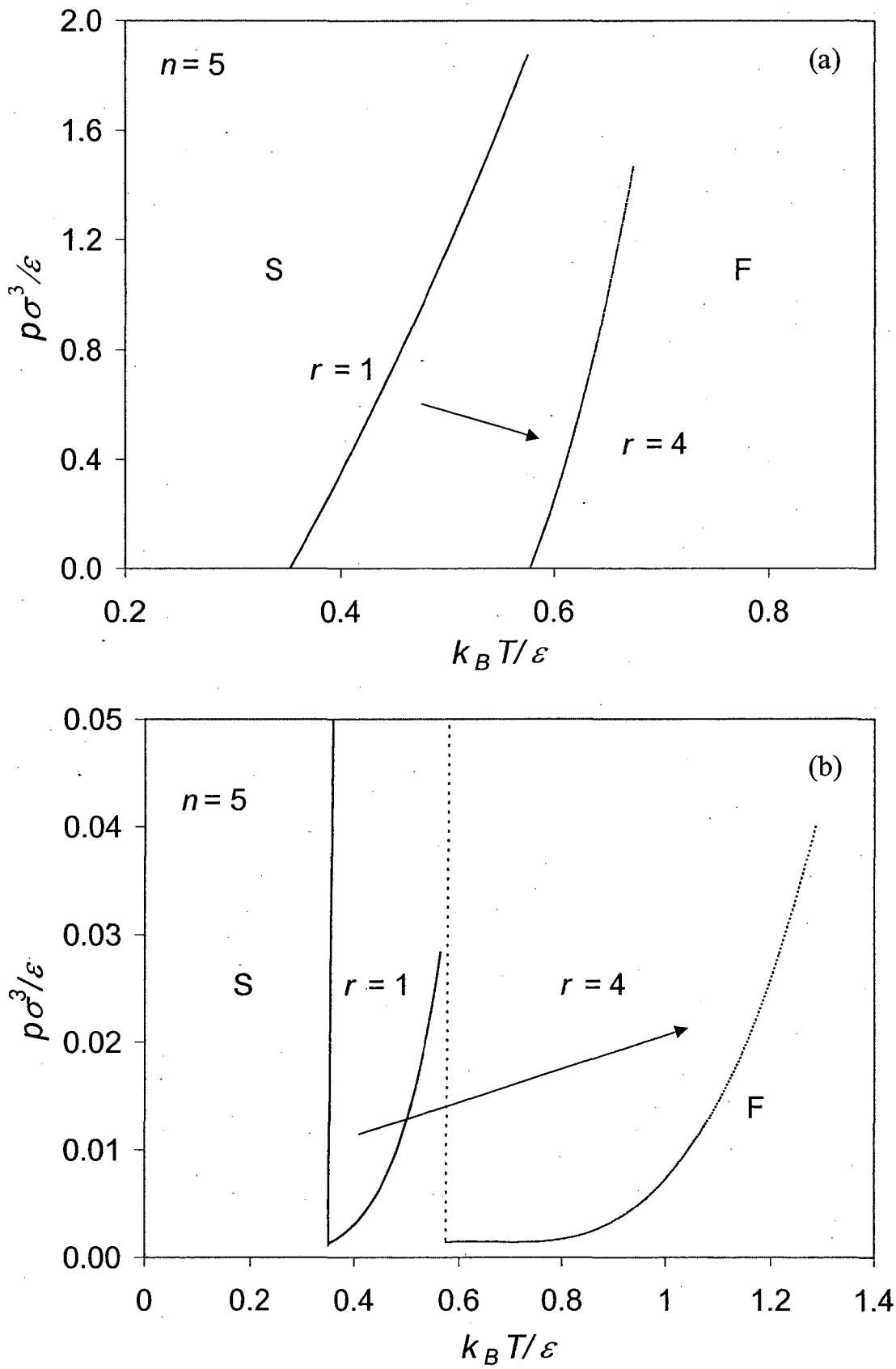
n = 5
(a)
S
F
r = 1
r = 4
2.0
1.6
1.2
0.8
0.4
0.0
0.2
0.4
0.6
0.8
$p\sigma^3/\varepsilon$
$k_B T/\varepsilon$
n = 5
(b)
S
r = 1
r = 4
F
0.05
0.04
0.03
0.02
0.01
0.00
0
0.2
0.4
0.6
0.8
1
1.2
1.4
$p\sigma^3/\varepsilon$
$k_B T/\varepsilon$

Figure 6

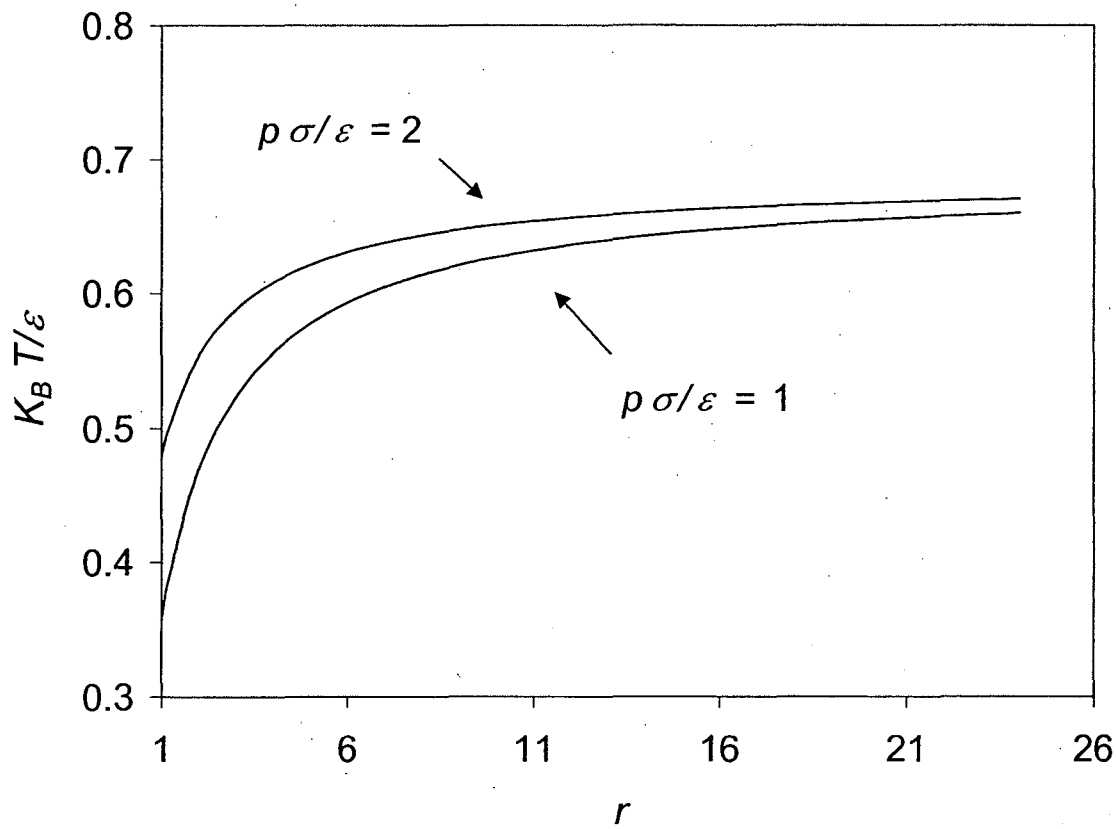
0.8
0.7
0.6
0.5
0.4
0.3
$K_B T/\varepsilon$
$p\,\sigma/\varepsilon = 2$
$p\,\sigma/\varepsilon = 1$
1
6
11
16
21
26
r

Ernest Orlando Lawrence Berkeley National Laboratory
One Cyclotron Road | Berkeley, California 94720

Prepared for the U.S. Department of Energy under Contract No. DE-AC03-76SF00098